IEEE Access
Multidisciplinary | Rapid Review | Open Access Journal

Received February 11, 2021, accepted March 2, 2021, date of publication March 10, 2021, date of current version March 18, 2021.

Digital Object Identifier 10.1109/ACCESS.2021.3065441

Mutual Coupling Reduction Using Ground Stub and EBG in a Compact Wideband MIMO-Antenna

AWAIS KHAN[1,2], SHAHID BASHIR[1], (Senior Member, IEEE), SALMAN GHAFOOR[3], AND KHURRAM KARIM QURESHI[4], (Senior Member, IEEE)

[1]Department of Electrical Engineering, University of Engineering and Technology, Peshawar, Peshawar 25000, Pakistan
[2]Department of Electrical Engineering, University of Science and Technology, Bannu, Bannu 28100, Pakistan
[3] School of Electrical Engineering and Computer Science, National University of Sciences and Technology (NUST), Islamabad 44000, Pakistan
[4]Optical Communications and Sensors Laboratory (OCSL), Electrical Engineering Department, King Fahd University of Petroleum and Minerals, Dhahran 31261, Saudi Arabia

Corresponding author: Awais Khan (engr_awais@yahoo.com)

The work of Khurram Karim Qureshi was supported by the Deanship of Research at King Fahd University of Petroleum and Minerals (KFUPM) under Project SB181022.

ABSTRACT This paper presents a compact, uni-planer wide band Multiple-Input-Multiple-Output (MIMO) antenna. The designed antenna array has a compact size of (26mm x 31mm) covering a wide frequency band from 3.1GHz - 11GHz. A partial ground plane shared by two radiating patches is used. A ground stub and a single column Electromagnetic Bandgap (EBG) structure in between the two radiating patches results in very low mutual coupling in the designed antenna. The proposed MIMO-antenna was evaluated through different performance metric indicators like channel capacity loss, far-field radiation pattern, S-parameters, envelope correlation coefficient, peak gain, diversity-gain and radiation efficiency. Our designed MIMO antenna has a very high isolation amongst the MIMO antennas ($S_{21} < -25$dB), a high Diversity-Gain (DG > 9.995 dB), a very low Envelope Co-relation Coefficient of (ECC < 0.001) and low Channel-Capacity-Loss (CCL < 0.1bits/s/Hz). The said antenna has an average radiation efficiency of 85.5% and a peak gain of (5.67dB) within the ultra-wideband (UWB) spectrum. A 0.8mm thick FR-4 substrate is used to fabricate the MIMO-antenna and tested in an anechoic chamber. The measured results closely match with the simulated results.

INDEX TERMS Channel capacity loss, electromagnetic band gap, envelope correlation coefficient, multiple input multiple output (MIMO), ultra wide band (UWB).

I. INTRODUCTION

Wideband antenna systems have got much consideration for use in recent wireless and mobile communications because of their high data-carrying capabilities, ease of fabrication, and cost-efficiency [1]. The Federal Communication Commission (FCC), in 2002 has reserved the frequency range of 3.1GHz to 10.6GHz for UWB applications. Due to its low transmission power and wide spectrum, UWB has many advantages: low power consumption and high immunity to signal interference. However, the efficiency and reliability of a UWB system is significantly affected by multi-path fading. To overcome this problem and enhance the UWB system performance, the MIMO technique has been introduced [2]. MIMO is a very efficient and reliable technique for modern wireless communication systems such as WLAN, 4G, and 5G communications. Since the MIMO technique involves multiple antennas that require more space for its implementation, the requirement of a compact MIMO structure has significantly increased for aesthetic and space saving reasons at both the mobile terminal and the base station [3].

Mutual coupling between individual radiating antennas is the main drawback with MIMO antenna systems which is dependent upon relative positions of the antenna elements i.e. the spacing between the elements. Therefore, an essential area of research is to minimize the mutual coupling in the design of a MIMO system [4]. Space radiation and surface waves are the two main causes of mutual coupling in an antenna array [5]. Various techniques have been proposed in the literature for the reduction of mutual coupling. For example, two parallel coupled-line resonators (PCRs) were used to increase the isolation in planar micro-strip patch antenna arrays [6]. In [7] both the causes of mutual coupling have been attempted. Frequency Selective Surface (FSS) wall

The associate editor coordinating the review of this manuscript and approving it for publication was Muhammad Zubair.

was inserted initially for suppressing the free space radiation among the Dielectric Resonator Antennas (DRAs). Further, the surface current was reduced by etching two different sized slots in the common ground plane, which was behaving like an LC resonator. The combination of FSS wall and the slots result in a very low mutual coupling of -30 dB. A new low pass filter with a wide stop-band made up of a Cross Shape Defected Ground Structure (CSDGS) was presented in [8], attaining a 20-dB isolation for the frequency range of 4.25–15.9 GHz. Another method proposed for reducing mutual coupling is using a complementary split-ring resonator (CSRR) at 25 GHz frequency [5], achieving -55dB isolation between the array elements.

A detailed study was presented in which different shapes of EBGs like square, triangular, circular, and hexagonal were discussed and their performances were analyzed [9]. It was noted that as long as the area of different shapes of EBGs remains identical, their performance remains similar. Mushroom type structure having vias between the ground plane and the patch can reduce mutual coupling between array elements if placed in between or surrounded by antenna elements [8]. Uni-planer compact EBG structures without vias that are easy to fabricate are also being used for increasing isolation among array elements [10], [11].Similarly, a Uni-planer Compact EBG (UC-EBG) gives high isolation between the antenna elements if used in combination with cross-shaped slots in the ground plane [12]. In [13], the Defected-Ground-Structure (DGS) is utilized for achieving a wide stop-band and decreasing the size of EBG elements. Similarly, a combination of tapered EBG and CSRR has also been used in [14] for obtaining a wide stop-band. Another tapered EBG and tapered DGS combination has been used in [15] to achieve a wide stop band.

A multi-period EBG structure can result in a broader stop-band than a single-period EBG. This technique combines the band gaps of two different period EBG structures by cascading them together and thus achieving a wider stop-band. The resulting multi-period EBG structure made by this method will remain uni-planer and thus attract filter designers [16].Another small size UWB MIMO antenna with the dimensions of $25 \times 25 \times 1.6$ mm^3, having cross shaped isolated ground stub and operating in 2.97-13.8GHz frequency band, is presented in [17]. The antenna has a high isolation ($S_{21} < -15$ dB), low ECC (< 0.05) and a high diversity gain ($DG > 9.97$).

Another highly isolated UWB MIMO antenna with a novel shape and smaller size of 50×30 mm^2 and having good diversity performance is presented in [1]. A stub similar to the shape of the letter "F" was inserted in the ground plane resulting in reduced mutual coupling among the two radiating patches. The presented MIMO antenna gives lower ($ECC < 0.04$), very high isolation of ($S_{21} < -20$dB), high peak gain, and higher diversity-gain ($DG > 7.4$dB) for the whole UWB band.

This paper presents the design of a novel compact MIMO antenna, operating in the UWB band with a much lower mutual coupling ($S_{12}/S_{21} < -25$dB) among its constituent patch antennas. The proposed design comprises two identical rectangular patch antennas with transmission line feed and having an inter-element spacing of 8mm. A combination of ground stub in bottom layer and an EBG structure in between the two rectangular patches in the top layer were used, resulting in very low mutual coupling among the two radiating patches. This antenna works in a wide frequency band of 3.1 to 11GHz and hence is a suitable candidate for use in WLAN, 5G (sub 6 GHz band), and satellite communications. The fabricated antenna has been tested for various parameters such as scattering parameters and radiation patterns, and a close resemblance is observed in experimental and simulated results.

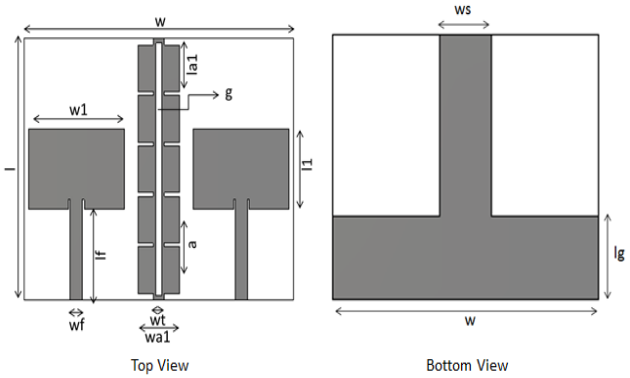

FIGURE 1. Proposed MIMO antenna.

II. ANTENNA DESIGN

Figure 1 shows the proposed MIMO antenna geometry. It consists of two identical rectangular patch antenna elements printed on a 26mm x 31mm and 0.8mm thick FR-4 substrate having a dielectric constant of 4.3. An inset feed-line is used for both the patch antennas to match with 50Ω characteristic line impedance. The feed line and two rectangular antennas are made on the top layer, whereas the ground plane, which is also shared between the two antennas, is made on the bottom layer of FR-4. There is only 8mm inter-element spacing between the two antennas, resulting in an overall compact design. The isolation between MIMO antenna elements is directly proportional to the separation between the antenna elements. Therefore, increasing the separation of the mutual coupling would reduce even more, but as one of the objectives of this research work is to design a compact MIMO antenna, increasing separation between the elements will increase the overall size of our antenna. Conversely, decreasing the separation further between the elements will increase mutual coupling, which is also against our primary objective of reducing it. It will also make it difficult to accommodate the EBG element in between the antenna elements. Therefore, 8mm separation is the optimized value for achieving both our objectives (compact size and low mutual coupling). A ground stub of width 'ws' and an EBG structure between the two rectangular patches on the top layer are used to reduce mutual

TABLE 1. Optimized parametric dimensions for designed MIMO antenna.

Parameters	Dimensions (mm)	Parameters	Dimensions (mm)
w	31	l1	8
l	26	gp	0.8
h	0.8	ws	6
lg	8.2	wa1	4.8
u	0.2	la1	4.6
v	1	a	5
wf	1.4	wt	1.3
lf	9	g	0.7
w1	11		

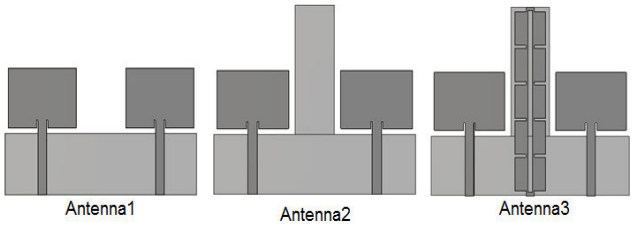

FIGURE 2. Modifications in the designed MIMO-antenna.

coupling among the two rectangular patches. Optimized parametric values for the proposed MIMO antenna are listed in Table-1.

The lower resonance frequency f_r of a rectangular microstrip patch antenna is calculated using equation 1 [18].

$$f_r = \frac{144}{lg + l1 + gp + \frac{w}{2\pi\sqrt{1+\varepsilon r}} + \frac{w1}{2\pi\sqrt{1+\varepsilon r}}} \text{GHz} \qquad (1)$$

The planar microstrip antenna is designed as per the above formula (1). Here "lg" represents the length of a ground plane, "$l1$" represents length of patch element and "gp" represents the separation gap between the ground plane and that of patch element. "w" and "$w1$" represent the width of the substrate and that of the patch element, respectively. By using values for the above parameters as given in Table-1, the calculated lower resonance frequency f_r is 7.25GHz, which is in agreement with the simulated resonance frequency of the microstrip antenna, as shown in Figure 3 (for antenna 1).

Figure 2 shows the evolution steps in the design process. Initially, only two identical rectangular patches were used with a shared partial ground plane (Antenna1) and analyzed for the desired results. Then a stub was introduced in the ground plane (Antenna2).

In the final step, an EBG column was inserted in between the two radiating elements (Antenna3) and tested for MIMO performances. Figure 3 shows the reflection and the transmission coefficients for Antenna1, Antenna2, and Antenna3, respectively. A low impedance bandwidth for antenna 1 gets improved in antennas 2 and 3, as shown in Figure 3 (i).

The small value of mutual-coupling among MIMO-antennas is always desirable for improved MIMO performances. Figure 3 shows a clear comparison of the coupling

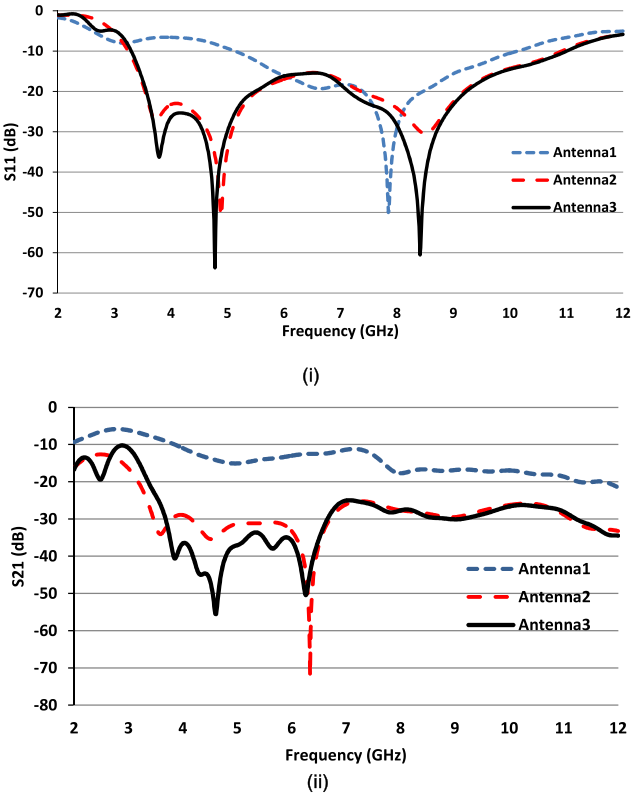

FIGURE 3. S-parameters (simulated), to demonstrate the effect of modifications (i) S11 (ii) S21.

level between all three antennas. Antenna1, having only a partial ground plane, shows a very high mutual coupling and is not a good choice for MIMO applications. In Antenna2, with the addition of a ground stub, the mutual coupling is decreased as compared to Antenan1. A further reduction in mutual coupling is observed with the addition of an EBG column between the two radiating elements (Antenna3).

A. EBG DESIGN AND ANALYSIS

Figure 4 shows evolutionary steps in the design of EBG structure. Initially, smaller unit cells of rectangular shapes are used in a vertical column with a period of a = 5mm (Figure 4 EBG-a), then a vertical strip is added, connecting all the unit cells in the middle (Figure 4 EBG-b) and finally, a vertical slot was created in that strip making it a single EBG column (Figure 4 EBG-c). The stepwise design of EBG (a, b, and c) was also analyzed for its frequency band rejection and was plotted as shown in Figure 4. The chosen EBG structure is simple, uni-planer (without having vias), and having small size, fulfilling our objective of a compact size MIMO antenna design.

The EBG was tested for its frequency rejection band using suspended transmission line analysis [19]. Figure 5 shows the effect of the number of EBG columns on the frequency band rejection and hence isolation between MIMO antennas. For this purpose, single, three, and five columns EBG were used and analyzed. The results showed an increase in isolation with

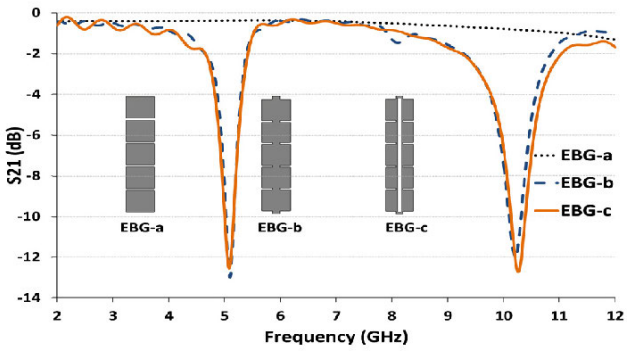

FIGURE 4. Steps in design of EBG.

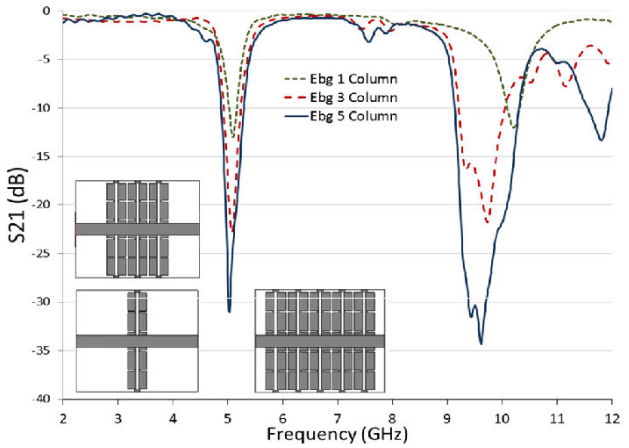

FIGURE 5. Effect of No. of EBG columns on Mutual coupling.

increasing the number of EBG columns, but in this paper, only a single column EBG has been used in order to achieve a more compact design.

The surface current distribution at different frequencies for all three antennas within the wide operating frequency band was analyzed. Figure 6 shows the current distribution plot for the three antennas at 3.89 GHz, 4.61GHz, 6.27GHZ and 9GHz when only port 1 of MIMO-antenna is excited. The color ramp in Figure 6 shows the intensity of surface /coupled current, where the red color shows the maximum intensity and the blue color shows the minimum current intensity. It can be clearly observed that in Antenna1, the coupled current for other radiator is very high. After the addition of the ground stub (Antenna2), the mutual coupling gets reduced. In Figure 6, it can be clearly observed that in Antenna3, when both the ground stub and EBG are used, the coupled current with the other radiator gets further reduced. Therefore, the mutual-coupling for the proposed MIMO-antenna (Antenna 3) is further reduced for all the given frequencies.

A parametric analysis is performed by varying the width "ws" of the ground stub for obtaining the optimized values; the results are shown in Figure 7. It can be seen in Figure 7 that keeping ws = 6 mm gives better results for reflection coefficient (S11) as well as isolation (S21).

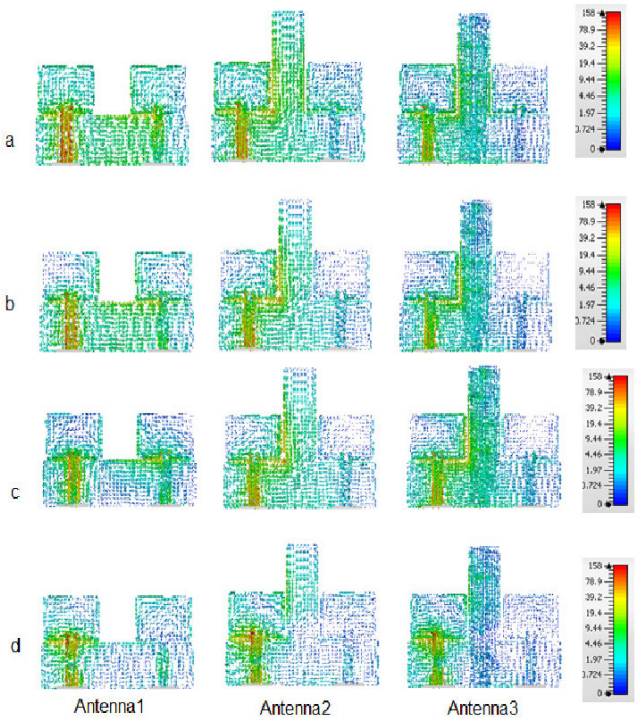

FIGURE 6. Surface currents (a) at 3.86 (b) at 4.61 (c) at 6.27 (d) at 9 GHz.

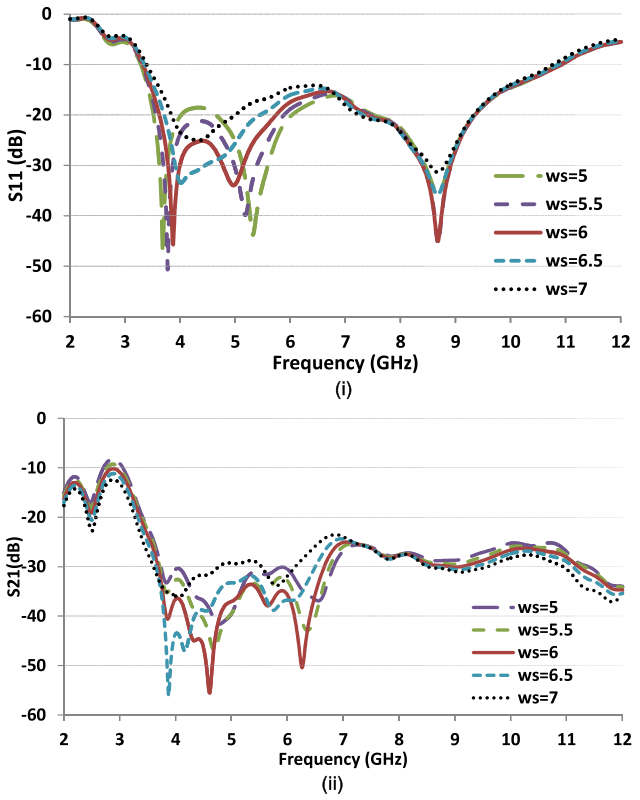

FIGURE 7. Effect of variation in width 'ws' of stub on (i) S11 (ii) S21.

III. RESULTS AND DISCUSSION

The proposed antenna was simulated and parameterized for optimized performance in CST. The optimized design was

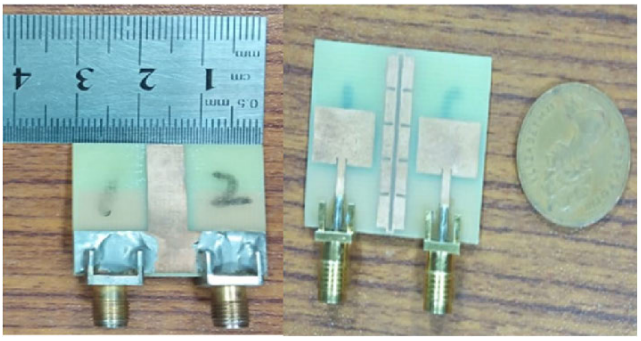

FIGURE 8. Photograph of fabricated MIMO antenna, top view (right) and bottom view (left).

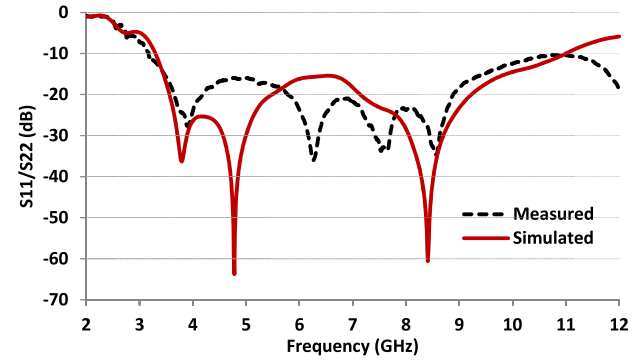

(i)

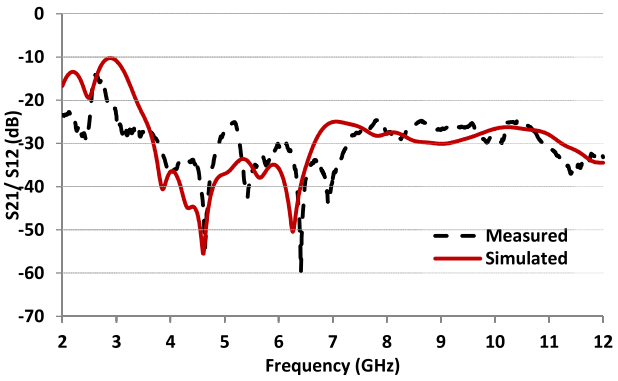

(ii)

FIGURE 9. Scattering parameters (Measured & simulated) of proposed MIMO-antenna (i) S_{11}/S_{22} (ii) S_{21}/S_{12}.

then fabricated to assess its measured performance. Picture of fabricated MIMO antenna is presented in Figure 8.

A. REFLECTION AND TRANSMISSION COEFFICIENTS

The fabricated antenna was tested for scattering parameters using a Network Analyzer. Figure 9 shows the plot of measured & simulated S parameters of the proposed design for comparison, indicating a good agreement with each other. The reflection coefficient ($S_{11}/S_{22} < -10$dB) and the transmission coefficient ($S_{21}/S_{12} < -25$dB) indicate acceptable impedance matching and improved mutual coupling reduction within the entire UWB band (3.1 GHz to 10.6GHz).

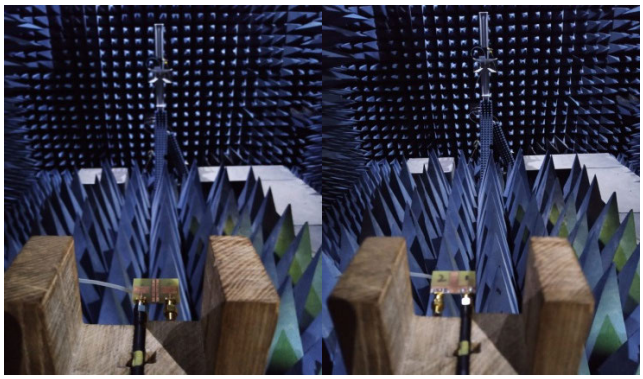

FIGURE 10. Proposed MIMO antenna testing for radiation pattern in anechoic chamber.

Small deviances among measured & simulated results are credited to the manufacturing /connections tolerance during the fabrication process.

B. RADIATION PATTERN

The designed MIMO antenna after fabrication was tested in an Anechoic chamber for radiation characteristics at different frequencies. Figure 10 shows the measurement setup inside the anechoic chamber for measuring radiation patterns. Measured and calculated radiation patterns are represented in Figure 11, showing azimuth plane (Left) as well as elevation plane (right) at 4, 7, and 10 GHz frequencies.

The experimental results for radiation pattern were obtained by exciting one of the ports (radiating element) while the other port was terminated with 50Ω load. An overall decent agreement is seen between the measured & simulated radiation patterns. Small disagreements between measured and simulated patterns are due to the constraints in the experimental setup, probable reflections from the terminated port and connector losses. It can be noted in Figure 11 that the pattern retains its shape in the elevation plane for all frequencies while the pattern shape changes slightly at higher frequencies in the azimuth plane.

C. ENVELOP CORRELATION COEFFICIENT

Envelop co-relation co-efficient is an essential parameter for the assessment of diversity performance of any MIMO antenna. There are mainly two methods used for calculating the ECC, one is based on the far-field pattern, which is very time-consuming and involves complex calculations, and the other one is from the scattering parameters of the antenna, which is a comparatively easy method. Therefore, the second method is adopted for calculating the ECC of the proposed antenna, as in [20].

$$ECC = \frac{\left|\mathbf{S}_{11}^{*}\mathbf{S}_{12} + \mathbf{S}_{21}^{*}\mathbf{S}_{22}\right|^{2}}{(\mathbf{1} - |\mathbf{S}_{11}|^{2} - |\mathbf{S}_{21}|^{2})(\mathbf{1} - |\mathbf{S}_{22}|^{2} - |\mathbf{S}_{12}|^{2})} \quad (2)$$

Ideally, the ECC should be 0 for an un-correlated MIMO antenna. However, the tolerable value is less than 0.5 for the actual MIMO antenna [21]. The proposed antenna has a

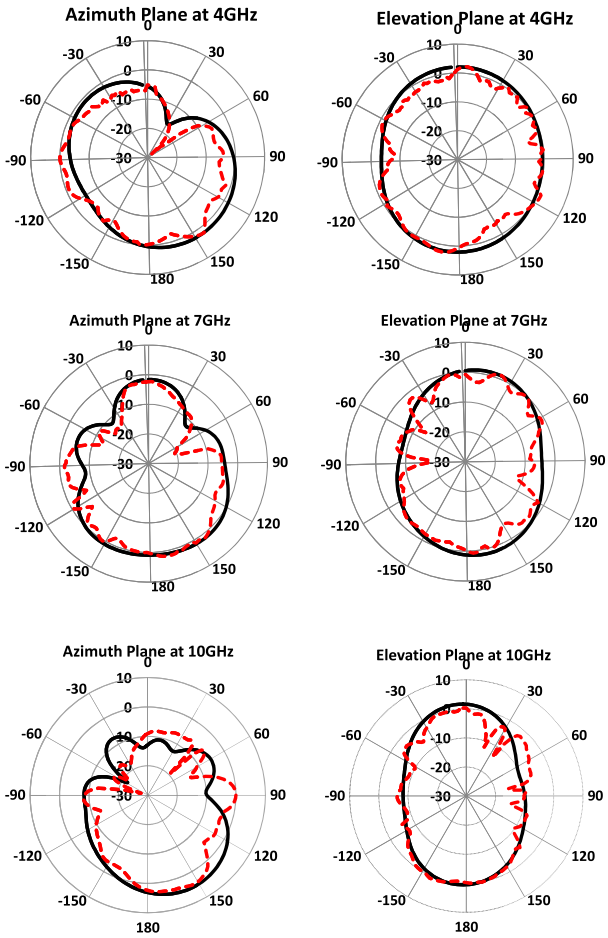

FIGURE 11. Simulation (—) & Measurements (----) results for Radiation-Pattern at 4, 7 & 10GHz.

computed ECC value of < 0.001 within its entire operating band, as displayed in Figure 12. Also, the simulated and measured ECC values are in close agreement. Hence the proposed compact MIMO antenna with such a small correlation between two antenna ports represents an excellent diversity performance.

D. DIVERSITY GAIN

Another significant MIMO performance indicator is diversity gain which can be calculated using the formula:

$$\mathrm{DG} = 10{*}\sqrt{(1 - \mathrm{ECC}^2)} \tag{3}$$

Diversity gain should be close to 10dB for satisfactory operation of MIMO antenna [21]. The plot of simulated and measured Diversity gain of the designed antenna matches well and is greater than 9.995 for the whole operating frequency band, as shown in Figure12.

Gain (simulated and measured) and efficiency plot is shown in Figure 13 for the proposed design, showing a 5.67dB peak gain and an average radiation efficiency of 85.5% for the UWB band of operation.

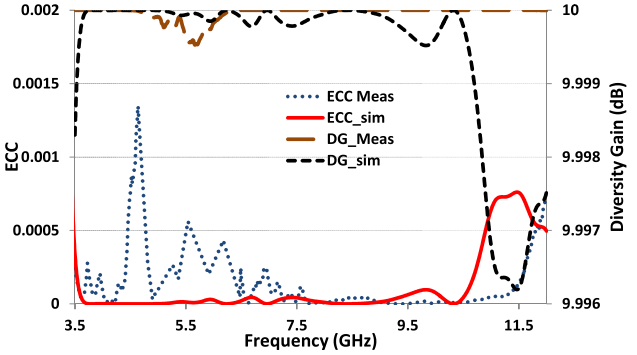

FIGURE 12. ECC of designed MIMO-antenna.

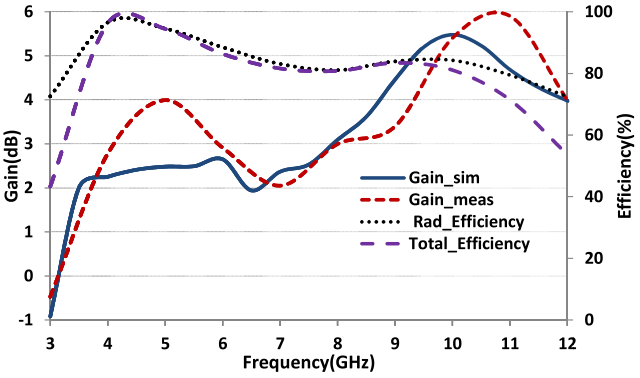

FIGURE 13. Peak Gain & Efficiencies for designed MIMO antenna.

E. CHANNEL CAPACITY LOSS (CCL)

The capacity of MIMO system increases with an increase in the count of antennas. However, the channel capacity losses also increase with it because of addition of correlation factor between the MIMO antenna elements. CCL value can be computed from equation (4), and it must be smaller then 0.4(bits/s/Hz) in order to achieve better MIMO diversity performance [29].

$$CCL = -log_2\left[det\left(\Psi^R\right)\right] \tag{4}$$

Here Ψ^R is a 2×2 co-relation matrix in terms of S- parameters, which may be written as:

$$\Psi^R = \begin{bmatrix} \varphi_{11} & \varphi_{12} \\ \varphi_{21} & \varphi_{22} \end{bmatrix}, \quad \text{and}$$

$$\varphi_{11} = 1 - (|S_{11}|^2 + |S_{12}|^2)$$

$$\varphi_{22} = 1 - (|S_{22}|^2 + |S_{21}|^2)$$

$$\varphi_{12} = S_{11}^* S_{12} + S_{21}^* S_{12}$$

$$\varphi_{12} = S_{22}^* S_{21} + S_{12}^* S_{21}$$

Figure 14 shows the calculated value of channel capacity loss which is well below 0.1(bits/s/Hz) for the entire operating band. Therefore, the proposed antenna has an excellent MIMO diversity performance.

F. PERFORMANCE COMPARISON

The designed MIMO antenna is compared for different performance metrics with recent related work published in

TABLE 2. Performance comparison with related published work.

Literature	Size (mm^2)	Band-width (GHz)	Isolation (dB)	Gain (dB)	CCL (bits/s/Hz)	ECC	Diversity Gain (dB)
[22]	25 x 32	3.1 -10.6	>20	--	--	< 0.05	> 9.99
[1]	50 x 30	2.5 - 14.5	>20	--	--	< 0.04	> 7.4
[23]	39 x 39	2.3–13.75	>22	< 4.6	<0.2	< 0.02	--
[24]	35 x 36	3.0 - 9	>17	--	<0.1	< 0.01	> 9.99
[25]	40 x 40	3.1 -10.6	>20	--	<0.2	< 0.04	--
[26]	26 x 26	2.9 - 11.6	>16	--	--	< 0.02	--
[17]	25 x 25	2.97 - 13.8	>15	--	--	< 0.05	> 9.97
[27]	40 x 43	3.1 - 10.6	>20	< 4	<0.3	< 0.02	--
[2]	31 x 26	3.1 - 11.2	>20	< 5	--	< 0.02	--
[28]	39 x 39	2.4 - 12.75	>15	< 5	--	< 0.02	--
This work	**26 x 31**	**3.1 - 11**	**>25**	**< 5.67**	**<0.1**	**< 0.01**	**> 9.99**

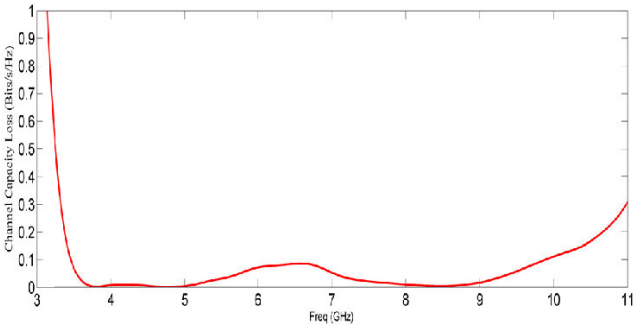

FIGURE 14. Channel Capacity Loss for proposed MIMO Antenna.

the literature as listed in Table2. The comparison is made based on channel capacity loss, area (size) of the antenna, the operating bandwidth, isolation level, peak gain, ECC, and diversity-gain. The proposed MIMO antenna achieves better isolation with a compact size, and therefore, it could be a suitable applicant for MIMO system applications.

IV. CONCLUSION

This paper proposes a compact size (26mm × 31mm) MIMO antenna for the UWB band with a very low mutual coupling ($S_{21/12} < -25$dB) within the whole operating band. The proposed technique uses a stub in the ground plane and a single column EBG structure between two rectangular patches. A peak gain of 5.67dB and 85.5% average radiation efficiency within UWB-band was obtained. After fabrication, the designed MIMO antenna was verified for S-parameters and radiation performance in an anechoic chamber. The measured results were in close agreement with simulated results, and the antenna has shown very decent MIMO diversity performance. A high diversity-gain (DG > 9.995), very low ECC < 0.001, and low channel capacity loss (CCL< 0.1bits/s/Hz) makes the designed MIMO antenna a suitable candidate for MIMO applications in the UWB band.

REFERENCES

[1] A. Iqbal, O. A. Saraereh, A. W. Ahmad, and S. Bashir, "Mutual coupling reduction using F-Shaped stubs in UWB-MIMO antenna," *IEEE Access*, vol. 6, pp. 2755–2759, 2018, doi: 10.1109/ACCESS.2017.2785232.

[2] A. Mchbal, N. Amar Touhami, H. Elftouh, and A. Dkiouak, "Mutual coupling reduction using a protruded ground branch structure in a compact UWB owl-shaped MIMO antenna," *Int. J. Antennas Propag.*, vol. 2018, pp. 1–10, Sep. 2018, doi: 10.1155/2018/4598527.

[3] M.-C. Tang, Z. Chen, H. Wang, M. Li, B. Luo, J. Wang, Z. Shi, and R. W. Ziolkowski, "Mutual coupling reduction using meta-structures for wideband, dual-polarized, and high-density patch arrays," *IEEE Trans. Antennas Propag.*, vol. 65, no. 8, pp. 3986–3998, Aug. 2017, doi: 10.1109/TAP.2017.2710214.

[4] M. S. Khan, A.-D. Capobianco, M. F. Shafique, B. Ijaz, A. Naqvi, and B. D. Braaten, "Isolation enhancement of a wideband mimo antenna using floating parasitic elements," *Microw. Opt. Technol. Lett.*, vol. 57, no. 7, pp. 1677–1682, 2015. [Online]. Available: https://onlinelibrary.wiley.com/doi/full/10.1002/mop.29162

[5] I. Nadeem and D.-Y. Choi, "Study on mutual coupling reduction technique for MIMO antennas," *IEEE Access*, vol. 7, pp. 563–586, 2019, doi: 10.1109/ACCESS.2018.2885558.

[6] K. S. Vishvaksenan, K. Mithra, R. Kalaiarasan, and K. S. Raj, "Mutual coupling reduction in microstrip patch antenna arrays using parallel coupled-line resonators," *IEEE Antennas Wireless Propag. Lett.*, vol. 16, pp. 2146–2149, 2017, doi: 10.1109/LAWP.2017.2700521.

[7] R. Karimian, A. Kesavan, M. Nedil, and T. A. Denidni, "Low-mutual-coupling 60-GHz MIMO antenna system with frequency selective," *IEEE Antennas Wireless Propag. Lett.*, vol. 16, pp. 373–376, 2017.

[8] H.-J. Chen, T.-H. Huang, C.-S. Chang, L.-S. Chen, N.-F. Wang, Y.-H. Wang, and M.-P. Houng, "A novel cross-shape DGS applied to design ultra-wide stopband low-pass filters," *IEEE Microw. Wireless Compon. Lett.*, vol. 16, no. 5, pp. 252–254, May 2006, doi: 10.1109/LMWC.2006.873594.

[9] S. M. S. Hassan and M. N. Mollah, "Identical performance from distinct conventional electromagnetic bandgap structures," *IET Microw., Antennas Propag.*, vol. 10, no. 12, pp. 1251–1258, Sep. 2016, doi: 10.1049/iet-map.2015.0697.

[10] B. Mohamadzade and M. Afsahi, "Mutual coupling reduction and gain enhancement in patch array antenna using a planar compact electromagnetic bandgap structure," *IET Microw., Antennas Propag.*, vol. 11, no. 12, pp. 1719–1725, Sep. 2017, doi: 10.1049/iet-map.2017.0080.

[11] M. J. Al-Hasan, T. A. Denidni, and A. R. Sebak, "Millimeter-wave compact EBG structure for mutual coupling reduction applications," *IEEE Trans. Antennas Propag.*, vol. 63, no. 2, pp. 823–828, Feb. 2015, doi: 10.1109/TAP.2014.2381229.

[12] X. Yang, Y. Liu, Y.-X. Xu, and S.-X. Gong, "Isolation enhancement in patch antenna array with fractal UC-EBG structure and cross slot," *IEEE Antennas Wireless Propag. Lett.*, vol. 16, pp. 2175–2178, 2017, doi: 10.1109/LAWP.2017.2703170.
[13] H. Zhu and J. Mao, "Miniaturized tapered EBG structure with wide stopband and flat passband," *IEEE Antennas Wireless Propag. Lett.*, vol. 11, pp. 314–317, 2012, doi: 10.1109/LAWP.2012.2191258.
[14] H.-R. Zhu, Y.-F. Sun, and X.-L. Wu, "A compact tapered EBG structure with sharp selectivity and wide stopband by using CSRR," *IEEE Microw. Wireless Compon. Lett.*, vol. 28, no. 9, pp. 771–773, Sep. 2018, doi: 10.1109/LMWC.2018.2853583.
[15] H. Rong, Q. Wang, S. Chen, Y. Cao, and H. Tian, "Wide stopband miniaturized 'I'-typed EBG with DGS," *Microw. Opt. Technol. Lett.*, vol. 60, no. 1, pp. 44–50, Jan. 2018, doi: 10.1002/mop.30910.
[16] C. C. Chiau, X. Chen, and C. Parini, "Multiperiod EBG structure for wide stopband circuits," *IEE Proc. Microw., Antennas Propag.*, vol. 150, no. 6, pp. 489–492, Dec. 2003, doi: 10.1049/ip-map:20031087.
[17] H. V. Singh and S. Tripathi, "Compact UWB MIMO antenna with cross-shaped unconnected ground stub using characteristic mode analysis," *Microw. Opt. Technol. Lett.*, vol. 61, no. 7, pp. 1874–1881, Jul. 2019, doi: 10.1002/mop.31792.
[18] K. G. Thomas and M. Sreenivasan, "Antenna with band dispensation," *IEEE Trans. Antennas Propag.*, vol. 58, no. 1, pp. 27–34, Jan. 2010.
[19] S. Ullah, W.-H. Yeo, H. Kim, and H. Yoo, "Development of 60-GHz millimeter wave, electromagnetic bandgap ground planes for multiple-input multiple-output antenna applications," *Sci. Rep.*, vol. 10, no. 1, pp. 1–12, Dec. 2020, doi: 10.1038/s41598-020-65622-9.
[20] N. Malekpour and M. A. Honarvar, "Design of high-isolation compact MIMO antenna for UWB application," *Prog. Electromagn. Res. C*, vol. 62, pp. 119–129, 2016, doi: 10.2528/PIERC15120902.
[21] G. Saxena, P. Jain, and Y. K. Awasthi, "High diversity gain MIMO-antenna for UWB application with WLAN notch band characteristic including human interface devices," *Wireless Pers. Commun.*, vol. 112, no. 1, pp. 105–121, May 2020, doi: 10.1007/s11277-019-07018-1.
[22] M. A. Ul Haq and S. Koziel, "Ground plane alterations for design of high-isolation compact wideband MIMO antenna," *IEEE Access*, vol. 6, pp. 48978–48983, 2018, doi: 10.1109/ACCESS.2018.2867836.
[23] Z. Tang, X. Wu, J. Zhan, S. Hu, Z. Xi, and Y. Liu, "Compact UWB-MIMO antenna with high isolation and triple band-notched characteristics," *IEEE Access*, vol. 7, pp. 19856–19865, 2019, doi: 10.1109/ACCESS.2019.2897170.
[24] J.-D. Park, M. Rahman, and H. N. Chen, "Isolation enhancement of wideband MIMO array antennas utilizing resistive loading," *IEEE Access*, vol. 7, pp. 81020–81026, 2019, doi: 10.1109/ACCESS.2019.2923330.
[25] S. Rajkumar, A. Anto Amala, and K. T. Selvan, "Isolation improvement of UWB MIMO antenna utilising molecule fractal structure," *Electron. Lett.*, vol. 55, no. 10, pp. 576–579, May 2019, doi: 10.1049/el.2019.0592.
[26] Z. Li, C. Yin, and X. Zhu, "Compact UWB MIMO vivaldi antenna with dual band-notched characteristics," *IEEE Access*, vol. 7, pp. 38696–38701, 2019, doi: 10.1109/ACCESS.2019.2906338.
[27] F. Amin, R. Saleem, T. Shabbir, S. U. Rehman, M. Bilal, and M. F. Shafique, "A compact quad-element UWB-MIMO antenna system with parasitic decoupling mechanism," *Appl. Sci.*, vol. 9, no. 11, p. 2371, Jun. 2019, doi: 10.3390/app9112371.
[28] S. R. Patre and S. P. Singh, "Shared radiator MIMO antenna for broadband applications," *IET Microw., Antennas Propag.*, vol. 12, no. 7, pp. 1153–1159, 2018, doi: 10.1049/iet-map.2017.0331.
[29] K. S. Sultan and H. H. Abdullah, "Planar UWB MIMO-diversity antenna with dual notch characteristicst," *Prog. Electromagn. Res. C*, vol. 93, pp. 119–129, 2019, doi: 10.2528/pierc19031202.

AWAIS KHAN received the B.Sc. and M.Sc. degrees in electrical engineering from the University of Engineering and Technology (UET), Peshawar, Pakistan. He is currently pursuing the Ph.D. degree in electrical engineering (communications) with the Department of Electrical Engineering, UET Peshawar. For eight years, he has worked as a Transmission Network Specialist with Telenor Pakistan. He is also a Lecturer with the Department of Electrical Engineering, University of Science and Technology, Bannu, Pakistan. His research interests include MIMO antennas, UWB antennas, and electromagnetic band gap materials.

SHAHID BASHIR (Senior Member, IEEE) received the B.Sc. degree in electrical engineering from the University of Engineering and Technology (UET), Peshawar, Pakistan, and the Ph.D. degree in wireless communications from the Department of Electronic and Electrical Engineering, Loughborough University, U.K., in 2009.

He is currently an Assistant Professor with the Department of Electrical Engineering, UET Peshawar, where he is a member of the National Center of Artificial Intelligence (NCAI) and the Centre of Intelligent Systems and Networks Research (CISNR). He has published his research in various reputed journals and conferences. His main research interests include wearable antennas, metamaterials, electromagnetic band gap materials, reconfigurable and miniaturized antennas for 5G, and THz antennas.

SALMAN GHAFOOR received the B.Sc. Electrical Engineering degree from the University of Engineering and Technology (UET), Peshawar, Peshawar, Pakistan, in 2006, the M.Sc. degree in electronic communications and computer engineering from the University of Nottingham, Nottingham, U.K., and the Ph.D. degree from the University of Southampton, Southampton, U.K. For two years, he was a Research Student with the Optoelectronics Research Centre (ORC), University of Southampton. In 2010, he joined the School of Electronics and Computer Science (ECS), University of Southampton, where he completed the Ph.D. degree, in 2012. He is currently an Associate Professor with the National University of Sciences and Technology (NUST), Islamabad, Pakistan. His research interests include free space optical communications, all-optical signal processing, ultra-wideband over fiber, and radio over fiber systems.

KHURRAM KARIM QURESHI (Senior Member, IEEE) received the B.Sc. (Hons.) degree in electrical engineering from the University of Engineering and Technology (UET), Lahore, Pakistan, in 1999, and the Ph.D. degree in electrical engineering from The Hong Kong Polytechnic University, in 2006. He is currently an Associate Professor with the Electrical Engineering Department, King Fahd University of Petroleum and Minerals (KFUPM). He has published more than 60 journal and conference papers and three US patents issued to his credit. His research interests include optical communications, optical signal processing, fiber and quantum dash lasers, optical sensors, and miniaturized antennas.